Biotechnology and Bioengineering

WILEY

BIOTECHNOLOGY AND BIOENGINEERING

ARTICLE

Peroxisome Engineering of *Yarrowia lipolytica* for Fatty Alcohol Production

Sivachandiran Somasundaram | Ayushi Agrawal | Philip Gitman | Michael Spagnuolo | Mark Blenner

Department of Chemical and Biomolecular Engineering, University of Delaware, Newark, Delaware, USA

Correspondence: Mark Blenner (blenner@udel.edu)

Received: 20 October 2025 | **Revised:** 9 January 2026 | **Accepted:** 27 January 2026

Keywords: compartmentalization | fatty alcohols | pathway localization | peroxisomes | *Yarrowia lipolytica*

ABSTRACT

Fatty alcohols currently find use in areas such as surfactants, plasticizers, lubricants, fuels, and the cosmetics industry; however, traditional production methods rely on non-renewable petroleum-derived compounds or are harvested from non-sustainable oil-seed crops. Recently, conventional hosts including *Escherichia coli* and *Saccharomyces cerevisiae* have been used for fatty alcohol production with some success. Oleaginous yeasts, such as *Yarrowia lipolytica*, offer significant advantages to produce oleochemicals, as their native metabolism evolved for high-flux fatty acid biosynthesis. However, fatty alcohol production in the cytosol faces challenges, including toxicity, limited availability of acyl-CoA, and the presence of competing pathways. To overcome these limitations, we targeted fatty alcohol biosynthesis into the peroxisome, where fatty acyl-CoA flux is naturally directed toward beta-oxidation and with fewer competing pathways. Following media optimization, fatty acyl-CoA reductases (FAR) from bacterial and mammalian sources were screened using canonical peroxisome targeting sequences. Additionally, we implemented an enzyme fusion strategy to physically colocalize FAR next to the 3-ketoacyl-CoA thiolase (3KAT) enzyme in the peroxisome. 3KAT fusion resulted in nearly double the titer of fatty alcohols, irrespective of which FAR was overexpressed. We then systematically engineered the subcellular environment within peroxisomes by increasing peroxisome numbers and boosting localized NADPH availability via the peroxisomal malate pathway and NADH kinase. These strategies significantly improved the organelle capacity for fatty alcohol production. The highest titer we achieved in shake flask culture was over 1.6 g/L of fatty alcohols. Further, we scaled up the fatty alcohol production in a 2 L bioreactor, achieved 2.77 g/L of fatty alcohols, in which a peak production of 2.53 g/L of C16:0 hexadecanol was achieved.

1 | Introduction

Fatty alcohols are oleochemicals with a wide range of applications in the cosmetics, detergents, and pharmaceutical industries (Keim 2013; Noweck and Grafahrend 2006). Currently, fatty alcohols are produced by oligomerization of fossil fuel-derived ethylene, followed by hydrogenation or from hydrogenation of non-sustainable palm oils (Munkajohnpong et al. 2020). Therefore, the development of a sustainable process to make fatty alcohols is needed. Fatty alcohols can be produced biologically in one of two ways, either by reduction of a fatty acyl-CoA or by the combined action of a carboxylic acid reductase and alcohol dehydrogenase on fatty acids (Akhtar et al. 2013; Fillet et al. 2015; Metz et al. 2000; Pollard et al. 1979). Based on the toxic effects of free fatty acids (Dulermo et al. 2015) and the availability of acyl-CoA, many studies favor the use of fatty acyl-CoA reductases (FARs) to catalyze fatty alcohol production (Bruder et al. 2019; Hofvander et al. 2011; A. Liu et al. 2013; Mehrer et al. 2018).

Yarrowia lipolytica is an oleaginous yeast that has naturally evolved to accumulate high lipid content directed through strong acetyl-CoA flux into fatty acid biosynthesis. Therefore, Yarrowia species are widely considered as a promising host for fatty alcohols production (Spagnuolo et al. 2019). Several studies have previously investigated *Y. lipolytica* for fatty alcohol

production. The expression of Fatty acyl-CoA reductase enzyme from *Tyto alba* (TaFAR) combined with increasing precursor supply in *Y. lipolytica*, achieved 690 mg/L of hexadecanol from shake-flask fermentation (Wang et al. 2016). Similarly, overexpression of fatty acyl-CoA reductase from *Marinobactor aquaeolei* VT8 (MaFAR) combined with a standard push-pull-block strategy achieved 557 mg/L of fatty alcohol in shake flask culture (J.-L. Zhang et al. 2019). More recently, combining high lipid flux strains of *Y. lipolytica* with overexpression of *MhFAR* from *Marinobacter hydrocarbonoclasticus*, achieved 1.1 g/L in shake flasks and 5.8 g/L of fatty alcohols from a bioreactor, in which oleyl alcohol (C18:1) was the major constituent (Cordova et al. 2020). In these studies, fatty alcohol production was directed to the cytosol; however, numerous competing pathways for fatty acyl-CoA and the potential toxicity of fatty alcohols may limit the titer and impact chain-specific alcohols distribution.

Compartmentalizing product pathways and co-localizing sequential reactions (sometimes referred to as substrate channeling) have been successful metabolic engineering strategies used to make several products (L. Chen et al. 2023; Sweetlove and Fernie 2018). The peroxisome is an organelle where beta oxidation occurs in yeast, in which fatty acyl-CoA chains (precursor of fatty alcohols) are shortened by two carbons per cycle of beta-oxidation and accumulate abundant acetyl-CoA flux. Several studies have examined the potential to use peroxisomes for compartmentalizing metabolic pathways to produce fuels, chemicals, and terpenoids (Baker et al. 2025; Bi et al. 2024; J. Gao and Zhou 2019; Hammer and Avalos 2017; C. Zhang et al. 2024; W. Zhou et al. 2025). In previous studies, peroxisomes were successfully harnessed in different host species such as *Saccharomyces cerevisiae*, *Pichia pastoris,* and *Ogataea polymorpha* to produce fatty alcohols (D'Espaux et al. 2017; N. Gao et al. 2022; Shen et al. 2024; Zhai et al. 2023). Particularly in the model host, *S. cerevisiae*, MaFAR was localized to the peroxisome resulting in 193 mg/L of fatty alcohol (Y. J. Zhou et al. 2016). Whereas, when TaFAR was localized to the peroxisome of *S. cerevisiae* along with additional engineering strategies, 1.3 g/L of fatty alcohol was produced in fed-batch fermentation (Sheng et al. 2016). Recently, peroxisome was engineered in methylotrophic yeast *O. polymorpha* by coupling both fatty alcohol biosynthesis and methanol utilization pathways in the peroxisome, resulting in titers of approximately 300 mg/L in shake flask batch cultures. The peroxisomal engineered strain shows a 3.9-fold increase in fatty alcohol production compared to cytosolic production (Zhai et al. 2023).

In a cell, organelle structures and metabolic functions have evolved to accommodate biochemical reactions for their own survival but may not be optimal to produce targeted products. To overcome these limitations, we implemented strategies to harness the peroxisome in *Y. lipolytica* to enhance the production of fatty alcohols. In this study, we systematically identified bottlenecks and increased the capacity of the peroxisomes to support higher production of compartmentalized fatty alcohols. We first tested a novel efficient peroxisome localization method and spatially organized the fatty alcohol biosynthetic pathway using an enzyme fusion strategy. Then, we systematically identified the bottlenecks in the peroxisomes and increased the peroxisomal localized redox power supply by overexpressing NADH kinase or auxiliary enzyme isocitrate dehydrogenase (IDP3) in the peroxisome. Next, we modulated the biogenesis of peroxisomes and increased the precursor fatty acid flux toward the production of fatty alcohols. Finally, our peroxisome-engineered strain was successfully scaled up in a 2 L bioreactor using bi-phasic extractive fermentation for 10 days and achieved a titer of 2.71 g/L of total fatty alcohol and the highest C16:0 hexadecanol fatty alcohol titer of 2.53 g/L to date.

2 | Materials and Methods

2.1 | Plasmid Construction

Construction of episomal expression cassettes: All plasmids used in this study were constructed using T4 ligation or sequence and ligation-independent cloning (SLIC) assembly methods (M. Z. Li and Elledge 2012). Leu2 and/or Ura3-based plasmids/cassettes were selected to construct the genes and transform the *Y. lipolytica* strain (Schwartz and Wheeldon 2018). All strains constructed in this study were listed in the Supporting Information S1: Table S1.

The genes *IDP3, tyPos5, PEX11, PEX16, ACL*, and *TGL4* were PCR-amplified from *Y. lipolytica* PO1f genomic DNA and cloned into either expression plasmid pIW245 (with Ura3 as selection marker) or pSL16 expression plasmid (with Leu2 as selection marker). Both plasmids encode for hrGFP with UAS1B8-TEF136 promoter and CYC1 terminator. All the genes were cloned into their respective episomal expression vectors using AscI/NheI digestion to replace hrGFP with genes using T4 DNA ligase which enabled the constitutive expression in *Y. lipolytica*. All the episomal expression plasmids constructed in this study are listed in Supporting Information S1: Table S2 and primers used to construct the plasmids are listed in Supporting Information S1: Table S3.

Construction of target genome integrative expression cassettes: CRISPR-Cas9 markerless integration Leu2 background plasmids pCRISPRyl_D17 and pCRISPRyl_AXP were used in this study for targeting the genomic loci in the *Y. lipolytica* strains (Schwartz et al. 2017). The genes *TaFAR*, *MaACR*, *MmFAR* were codon optimized for *Y. lipolytica* expression and synthesized by Genscript (Supporting Information S1: Table S4). The genes were PCR amplified and fused with PTS1 tags (AKL, SKL, BNICL), PTS2 tag, and *3KAT* gene using overlap extension PCR (Bryksin and Matsumura 2010). All fusion gene constructs were cloned into the homology donor URA3 background plasmids pHR_D17_*hrGFP* and pHR_AXP_*hrGFP* using AscI/NheI digestion and replace *hrGFP* with the respective fusion gene using T4 DNA ligase for ligation. Target genome integrative plasmids cassette constructed in this study are listed in the Supporting Information S1: Table S2. These co-expression plasmids enabled integrative selection with leucine and uracil auxotrophy and expression of enzymes at the target loci in the genome. Further, subsequent curing procedures have removed both leucine and uracil markers present in the cells. CRISPR-Cas9-based knockout plasmids pCas9-Leu and pCas9-Ura were used to construct the double-cut knockout system (D. Gao et al. 2018). Knockout plasmids were generated using SLIC by insertion of two annealed oligonucleotides containing gene target sequences of gRNAs and SLIC overhangs into the parent plasmid digested with NsiI. The knockout plasmids constructed in this study are presented in Supporting Information S1: Table S2.

2.2 | *Y. lipolytica* Strains Construction

In this study, *Escherichia coli DH5α* cells were used for plasmid construction and cultured in LB (Luria-Bertani) medium at 37°C at 250 rpm with 100 mg/L ampicillin to maintain the plasmids. YPD media was used to generate frozen stocks and preparing cells for transformation containing 10 g/L yeast extract, 20 g/L peptone, and 20 g/L glucose. All constructed episomal expression vectors or markerless genome-targeted integration plasmids were transformed into *Y. lipolytica* PO1f cells using the lithium acetate method. *Y. lipolytica* strains were plated on solid YPD medium and incubated at 30°C for 24 h. Fresh one-step buffer was prepared as follows: 90 μL of 50% PEG 4000 (sterile filtered), 5 μL of 2 M lithium acetate (sterile filtered), 2.5 μL of salmon sperm DNA (ssDNA was boiled at 98°C for 10 min), and 2.5 μL of 2 M dithiothreitol (DTT). A loop full of *Y. lipolytica* cells were taken and mixed with the one-step buffer. Then, 250−500 ng of plasmid DNA was added to the tube containing one-step buffer and cells, which was then mixed and vortexed for 10 s. The tubes were then incubated at 39°C in a water bath for 1 h to facilitate the transformation of plasmids into the cells. After incubation, 100 μL of the transformation mixture was plated on its respective YSC selective plates and incubated at 30°C for 2 days.

Multiple colonies obtained from the YSC selection plates were screened using colony PCR targeting the insert with a gene-specific primer set for episomal strains. In case of genome integration, colonies exhibiting positive integration of genes were cured for the two plasmid marker system by growth in rich YPD media supplemented with 5-fluoroorotic acid (5-FOA) (Schwartz and Wheeldon 2018). Final engineered markerless strains were confirmed by PCR fragment size with gene-specific primers and subsequently verified by Sanger sequencing.

2.3 | Visualization of Enzyme Localization Using Fluorescence Microscopy

To confirm whether 3-ketoacyl-CoA thiolase (3KAT) enzyme is effectively localizing TaFAR into the peroxisomes, Green Fluorescent Protein (GFP) from *Humanized renilla* was fused at the C-terminus of 3KAT using the flexible linker $(GGGS)_3$ and then the cassettes were transformed into the *Y. lipolytica* strain PO1f. Cells expressing GFP in the cytosolic space were used as a control strain for a non-localization target. Both strains were grown for 48 h in YSC drop-out media containing 20 g/L glucose at 30°C and 220 rpm. GFP localization was assessed using a Zeiss LSM 880 confocal microscope with a ×63/1.4 objective. GFP was excited at 488 nm and its fluorescence collected above 500 nm.

2.4 | Flask Fermentation for Biphasic Cultivation of Fatty Alcohol

Primary cultures of engineered *Y. lipolytica* strains for tube fermentation prepared in 14 mL culture tubes containing 2 mL of YSC drop-out media incubated at 30°C and 220 rpm. *Y. lipolytica* cells were inoculated from 48 h precultures to shake flasks cultivation at an initial cell density of 0.2 at 600 nm (OD600) at 220 rpm and 30°C for 7 days of flask fermentation. All engineered strains for fatty alcohol production were cultivated in 125 mL baffled flasks containing 12 mL defined YSC drop-out media containing 6.7 g/L Yeast Nitrogen Base (without ammonium sulfate), 1.365 g/L ammonium sulfate, and 0.69 g/L of CSM-leu and/or CSM-Ura in 80 g/L of glucose as the sole carbon source.

Continuous extractive fermentation was performed in shake flask cultivation to extract the fatty alcohols production from engineered strains by adding dodecane (Sigma) as overlay (Wang et al. 2016). The impact of dodecane on cell growth was initially assessed by the addition of dodecane at different time points in cell growth (data not shown). To minimize the impact of dodecane on the growth of engineered *Y. lipolytica* strains, we added 3 mL of dodecane overlay in 12 mL of cells at 36 h for the continuous extraction of fatty alcohols and maintained a biphasic culture as aqueous:organic emulsion throughout the flask fermentation.

2.5 | Fed-Batch Fermentation in Bioreactor for Fatty Alcohol Production

Based on our extractive flask fermentation results, we selected the best Fatty alcohol production strain FS113 to scale up in a 3 L Eppendorf BioFlo 320 bioreactor with the addition of a 10% dodecane extractive layer. The seed strain was inoculated in 250 mL YSC drop-out media and grown overnight. The initial cell density of 0.15 OD_{600} of inoculum from the seed culture was loaded in a total operating volume of 2 L in a bioreactor with the media containing 80 g/L glucose, 6.7 g/L Yeast Nitrogen Base, 0.69 g/L CSM-Leu-Ura, and 1.365 g/L ammonium sulfate. Dissolved oxygen (DO) was maintained at 40% by stirring agitator from 300 to 800 rpm via primary cascade and pH was maintained to 5.0 by auto-dispensing a base solution of 3 M NaOH (Cordova et al. 2020; D'Espaux et al. 2017; Fillet et al. 2015). At 72 h of culture, the first glucose pulse of 80 g was added to the bioreactor (Stock concentration of 600 g/L). To prevent glucose exhaustion and maintain the cells in the active lipogenesis phase, we added a second glucose pulse of 80 g at approximately 144 h. Temperature was maintained at 30°C using the reactor water jacket and continuously sparging air into the bioreactor at a rate of 0.2−2.5 splm. 5% v/v of sterile antifoam 204 (Sigma) was added when necessary during the run. A fermentation run in a bioreactor was carried out for 10 days, and samples were collected each day for analysis. Dry cell weight was determined for 1 mL of cells by double washing in PBS and dried the residual liquid at 80°C for > 30 min. Samples obtained at different time points during the bioreactor run were quantified for glucose, citrate, and profiled for lipids and alcohols in duplicates.

2.6 | Extraction and Quantification of Fatty Alcohols

Five hundred microliters of top overlay broth from the fermentation cultures was taken and centrifuged at 10,000×*g* for 10 min and carefully pipetted out the dodecane overlay to quantify the fatty alcohol concentration. The concentration of fatty alcohols from the dodecane overlay was analyzed by Trace 1310 Gas Chromatography (TermoFisher Scientific) equipped with Flame Ionization Detection system (FID, ThermoFisher

Scientific) and DB-WAXETR (Agilent) 30 m, 0.25 mm, 0.25 μm, JW GC column. The injected volume of the sample was 1 μL (split ratio of 5) with the flow rate of 1 mL/min. The initial oven temperature was set at 50°C and ramped to 150°C at a ramp rate of 25°C/min and maintained for 2 min, followed by ramping the oven temperature to final 250°C at the ramp rate of 4.0°C/min to the total run time for 41 min.

2.7 | Extraction and Quantification of Fatty Acids Methyl Esters (FAMEs)

To quantify the fatty acid concentration, 1 mL of cells was collected from the fermentation and centrifuged at 4500 × *g* for 5 min. Cell pellets were added with 100 μL of internal standard (IS) solution (2 mg/mL methyl pentadecanoate and 2 mg/mL glyceryl triheptadecanoate) and resuspended with 500 μL 0.5 N sodium methoxide (20 g/L sodium hydroxide in methanol). Cells were vortexed for 40 min at 2000 rpm on a heavy-duty vortexer. Forty microlitres of concentrated sulfuric acid were directly added to the tubes. Further, 850 μL of hexane was added to the tubes to neutralize the samples and vortexed at 2000 rpm for 20 min on a heavy-duty vortexer. Finally, the samples were centrifuged for 1 min at maximum rpm to obtain the hexane layer containing FAME's. FAME analysis was performed by GC-FID in DB-23 (Agilent) 30 m, 0.25 mm, 0.25 μm column. The GC program was as follows: Initial oven temperature of 50°C and ramped to 175°C at the ramp rate of 25°C/min and maintained for 1 min, followed ramping the oven temperature to 230°C at the ramp rate of 4.0°C/min and hold for 5 min, then final ramping to 250°C at the ramp rate of 25°C and hold it for 2 min.

2.8 | Extraction and Quantification of Glucose and Citrate

The glucose and citrate time profile in the fed-batch bioreactor run was determined by High Performance Liquid Chromatography (HPLC). One milliliter of the aqueous phase broth sample was taken at different time points during the bioreactor run and centrifuged at 12,000 × *g* for 10 min. The supernatant after centrifugation was filtered through a 0.22-μm syringe filter and analyzed with an Aminex HPX-87H column (Bio-Rad) on a 1290 Infinity II HPLC (Agilent), which is equipped with a Refractive Index Detector (RID). Glucose and citrate were eluted with 5 mM H_2SO_4 (sulfuric acid) as the mobile phase solvent at a flow rate of mobile phase was 0.6 mL/min at 50°C for 30 min. The standard curve for glucose and citrate was obtained using the same procedure.

3 | Results and Discussion

3.1 | Construction, Optimization, and Localization of Fatty Alcohol Biosynthetic Enzymes Using PTS1 Signals

The biosynthetic production of metabolites in yeast is often limited by the toxicity of intermediate products and the formation of byproducts by competing endogenous pathways. To address this limitation, we aimed to harness the peroxisome for fatty alcohol production using Peroxisome Target Signal Type 1 (PTS1). Initially, we constructed a base strain, termed FS100, in *Y. lipolytica* Po1f by knocking out the *FAA1* (Fatty Acid Activation) and *FAO1* (Fatty Alcohol Oxidase) genes using CRISPR-Cas9 in order to avoid the common fatty alcohol degradation pathways (Supporting Information S1: Figure S1) (Gatter et al. 2014). Further, various strategies were applied in FS100 to build all the fatty alcohol producing strains presented in this work (Figure 1). Based on previous studies (Q. Gao et al. 2020; Youngquist et al. 2013), we first selected three different fatty acyl reductase (FAR) enzymes such as TaFAR, MaACR, and MmFAR from *T. alba*, *M. aquaeolei*, and *Mus musculus*, respectively. These enzymes were successfully localized to the peroxisome by fusing them to a non-canonical PTS1 tag BNICL from *Brassica napus*, resulting in the strains FS101, FS102, and FS103 for the compartmentalized production of fatty alcohols. Among the tested strains, FS101 expressing TaFAR had the highest total fatty alcohol titer of 40 mg/L (Supporting Information S1: Figure S2a).

We next sought to optimize our media conditions. Lipid accumulation in *Y. lipolytica* is tightly coupled with depletion of environmental nitrogen in the presence of excess carbon (Pomraning et al. 2016). Therefore, we aimed to improve fatty alcohol production through upregulating precursor fatty acid flux by implementing nitrogen-limited media. The fatty alcohol-producing strain FS101 was tested in different C/N ratios, including 40:0.25, 40:0.68, 40:1. 40:1.5, 40:2.5, 40:3.5 (Blazeck, Hill, et al. 2014). Among the tested C/N ratios, the media containing a 40:0.68 ratio (80 g/L glucose and 1.36 g/L ammonia sulfate) showed the highest fatty alcohol production by increasing the fatty acid precursors.

To further improve the peroxisomal localization efficiency, we selected other commonly used PTS1 signal tags and constructed the strain FS104 by fusing the amino acid sequence alanine–lysine–leucine (AKL) to the C-terminus of TaFAR and strain FS105 by fusing serine–lysine–leucine (SKL) to the C-terminus of TaFAR. We then tested the strains FS101, FS104, and FS105 containing TaFAR with three different PTS1 signal tags, BNICL, AKL, and SKL, in the C/N optimized media for 7 days in flask culture. The strain in which TaFAR was localized to peroxisome via SKL (FS105) produced the highest titer of 452 mg/L fatty alcohols, in which 88% of the alcohol is C16:0 and 12% is C18:0. (Supporting Information S1: Figure S2b). The AKL construct has produced the second-highest titer of 374 mg/L fatty alcohols, whereas the BNICL construct produced only 77 mg/L. Despite the BNICL working better to effectively localize other enzymes in peroxisomes (data not published), it was the least effective for FARs to localize in peroxisomes in this study.

3.2 | 3KAT-Directed Compartmentalization Enhances Peroxisome Localization for Fatty Alcohol Production

Next, we attempted to co-localize the fatty alcohol biosynthetic pathway in close proximity to the beta oxidation pathway, where acetyl-CoA would be abundant in the peroxisome. We hypothesized that co-localization of FARs with the beta oxidation enzymes would give the FARs more access to acyl-CoA

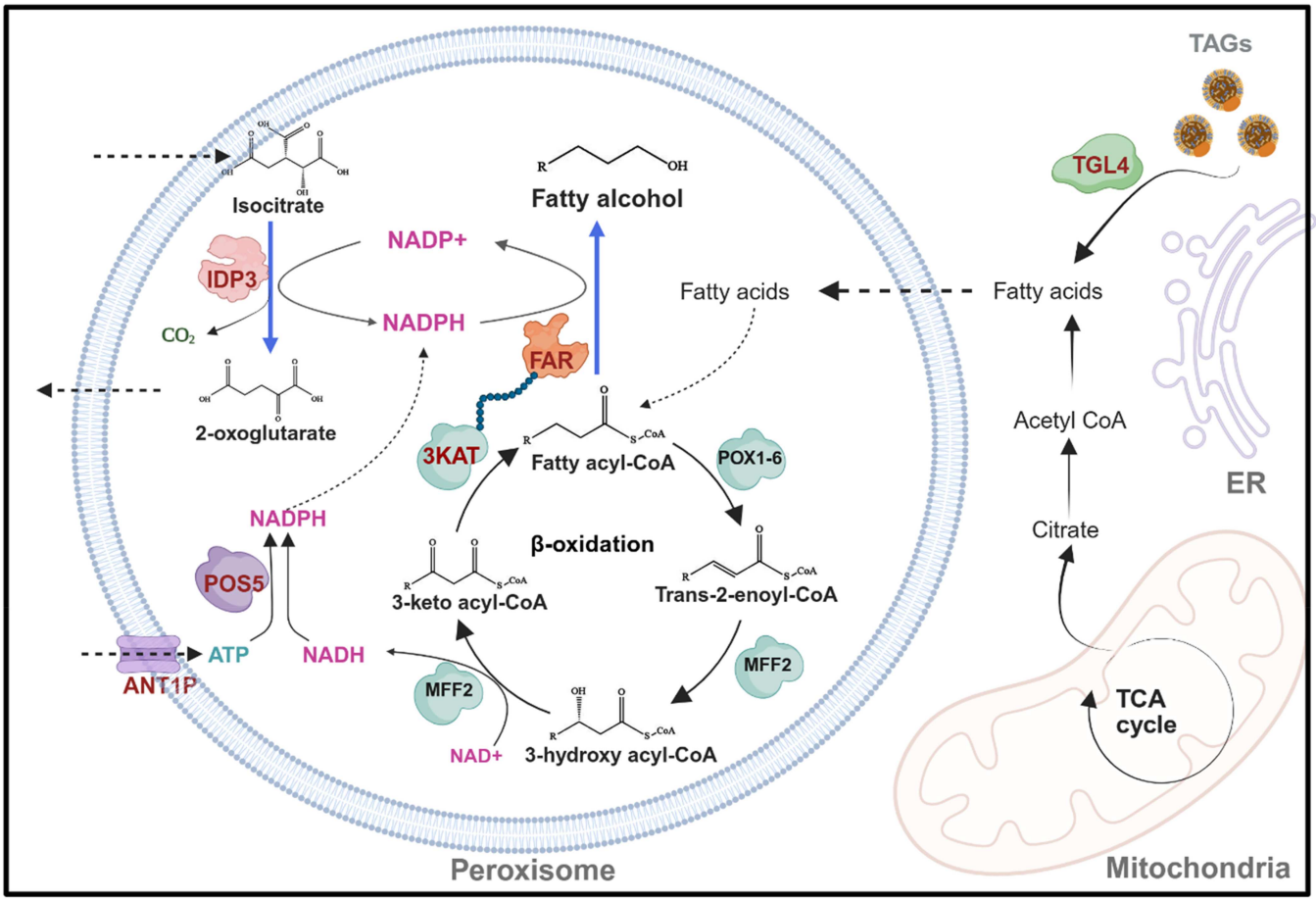

FIGURE 1 | Schematic diagram shows different strategies implemented in the peroxisomes to improve the compartmentalized production of fatty alcohol in *Yarrowia lipolytica*. The enzymes overexpressed in this study are highlighted in red text.

substrates, thereby improving fatty alcohol production. To achieve this, we constructed enzyme fusion complexes consisting of non-native FARs (TaFAR, MaACR, MmFAR) fused to the C-terminus of 3KAT (also known as POT1), a native peroxisomal enzyme involved in beta-oxidation (Figure 2a). Strains were engineered to express FARs fused to the C-terminus of 3KAT using either a flexible GS linker (GGGGSGGGGSGGGGS; FS106) or a rigid EF linker (GSAGSAAGSGEF; FS107) (Figure 2b). Expression of 3KAT-TaFAR fused via the flexible GS linker by strain FS106 produced fatty alcohols at 693 mg/L, whereas expression of 3KAT-TaFAR fused via the rigid EF linker by strain FS107 produced fatty alcohols at 475 mg/L. Likewise, strains expressing the 3KAT-MaACR (FS108) and the 3KAT-MmFAR (FS109) fusion proteins connected via a flexible linker produced total fatty alcohols at 211.7 and 657 mg/L, respectively (Figure 2d).

To test the efficiency of peroxisome localization, 3KAT was fused to an hrGFP reporter (FS110) and examined under confocal microscopy in comparison with cytosolic expression of GFP (FS111) (Figure 2c, left panel). The confocal images show clear localization of GFP in puncta characteristic of peroxisomes (Figure 2c, right panel). Further, we used the protein localization prediction tool WoLFPSORT (https://wolfpsort.hgc.jp/), and identified the presence of a native peroxisome target signal type 2 (PTS2) tag at the N-terminus of 3KAT, a 9-amino acid peptide at the N-terminus that naturally helps the enzyme localize into the peroxisomes. To determine whether the PTS2 tag from 3KAT alone was sufficient for enabling fatty alcohol production in peroxisomes, we constructed strain FS112 expressing PTS2 directly fused to the N-terminus of TaFAR. Our results show the greatest titer enhancement is achieved through the fusion to 3KAT compared to the use of PTS2 alone (Figure 2d), thus confirming the critical role of 3KAT-fusion in enhancing compartmentalized production of fatty alcohols in peroxisomes. As a comparison, we constructed strain FS127 expressing TaFAR in the cytosol, showing similar results (Supporting Information S1: Figure S2b). While cytosolic expression provided a useful comparison, the central objective of this study was to enhance peroxisomal fatty alcohol production. Therefore, our subsequent efforts focused on peroxisomal engineering strategies.

3.3 | Enrichment of Localized NADPH Redox Supply in Peroxisomes

Next, we systematically identified the bottlenecks in the peroxisome to increase its capacity for fatty alcohol production. Fatty alcohol biosynthesis from fatty acyl-CoA is carried out by a two-step reduction reaction, which requires two NADPH cofactors to drive the reduction reaction by FARs enzyme. The peroxisome contains an endogenous auxiliary enzyme IDP3 to catalyze the reaction of isocitrate to α-ketoglutarate and reduced cofactor NADPH, which is essential to the 2,4-dienoyl-CoA reductase

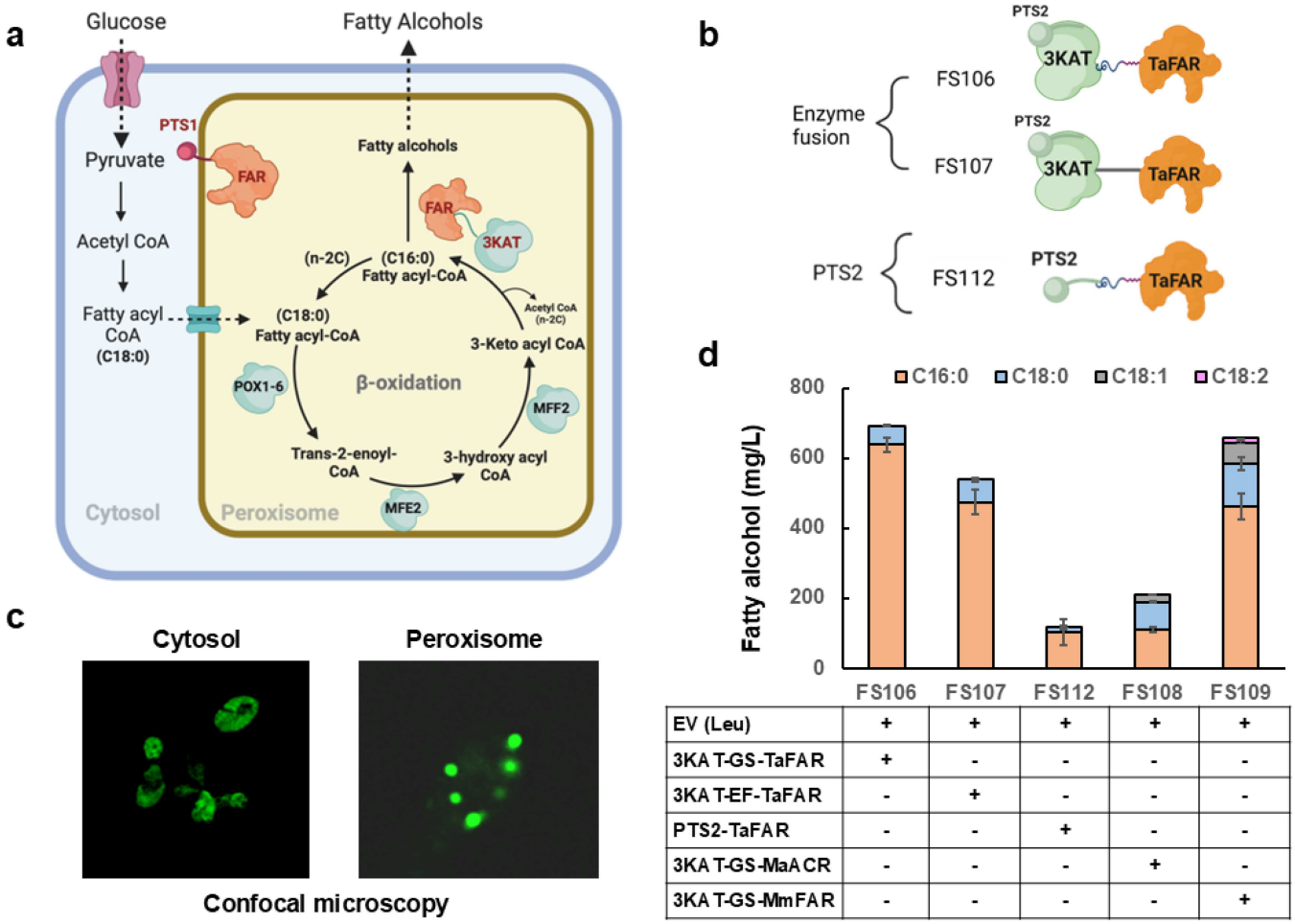

	FS106	FS107	FS112	FS108	FS109
EV (Leu)	+	+	+	+	+
3KAT-GS-TaFAR	+	-	-	-	-
3KAT-EF-TaFAR	-	+	-	-	-
PTS2-TaFAR	-	-	+	-	-
3KAT-GS-MaACR	-	-	-	+	-
3KAT-GS-MmFAR	-	-	-	-	+

FIGURE 2 | Localization and production of fatty alcohol in peroxisome. (a) Schematic diagram of the localization of fatty alcohol biosynthetic enzyme in the peroxisome using the PTS1 and 3KAT enzyme fusion strategies. (b) Cartoon representation of the peroxisome signal tags and the 3KAT-FAR enzyme fusions utilized by strains FS106, FS107, and FS110. (c) Multiple cell image of *Yarrowia lipolytica* strain FS111 shows GFP localization in the cytosolic space (left panel), a single cell image of *Y. lipolytica* strain FS110 shows localization of GFP in the peroxisome using the 3KAT fusion system (right panel). (d) Fatty alcohol production from various 3KAT fusion strains with Empty vector, contain leucine biosynthesis (EV(leu)).

enzyme for the degradation of polyunsaturated fatty acids with double bonds at even-numbered positions (Rottensteiner and Theodoulou 2006) (Figure 3a). To assess if alcohol production is limited by peroxisomal redox power, exogenous isocitrate was supplied directly to the strain FS101, which showed improvement in fatty alcohols titer (Supporting Information S1: Figure S3a). Therefore, we hypothesized that the peroxisomal NADPH/$NADP^+$ ratio could contribute to the rate limitation in FAR-driven peroxisomal fatty alcohol biosynthesis. Thus, we constructed a strain (FS113) that overexpresses the endogenous auxiliary enzyme IDP3 in FS106 background to improve the NADPH pool in the peroxisomes, resulting in 1.25 g/L of fatty alcohols (Figure 3b). IDP3 is known to produce NADPH in the peroxisomes of *S. cerevisiae*. To test if IDP3 is the major source of NADPH in *Y. lipolytica*, strain FS114 was constructed in which IDP3 was knocked out, and a growth challenge experiment was performed on a polyunsaturated fatty acid as the sole carbon source. FS114 had severely impaired the growth in linoleic acid compared to FS106 (Supporting Information S1: Figure S3b), suggesting that IDP3 is the major NADPH supplier in *Y. lipolytica* peroxisomes and that diffusion of NADPH across the membrane did not occur. To further increase the redox supply in the peroxisome, we knocked out the gene encoding 2,4-dienoyl-CoA reductase, which competes with TaFAR for NADPH in the peroxisomes resulting in the strain FS115. The knockout was confirmed through sequence verification and a growth challenge experiment. The strain FS115 exhibited impaired growth when linoleic acid was used as the sole carbon source but grew well when glucose was used as the sole carbon source (Supporting Information S1: Figure S3b). Contrary to our expectations, fatty alcohol production was completely abolished in the strain FS115.

As an alternative route to increase the peroxisomal NADPH, we localized the NADH kinase from *Y. lipolytica* to the peroxisome to convert ATP and beta oxidation-derived NADH into NADPH (Figure 3a). In *S. cerevisiae*, the NADH kinase POS5 performs this reaction using NADH localized in the mitochondrial matrix with a low K_m of 0.49 mM (Outten 2003). We identified a *Pos5* homolog (*ylPos5*) in the *Y. lipolytica* genome, which also contains a mitochondrial signal peptide at its N-terminus. We truncated the mitochondrial localization signal peptide to obtain a truncated POS5 (tylPos5) enzyme, and fused

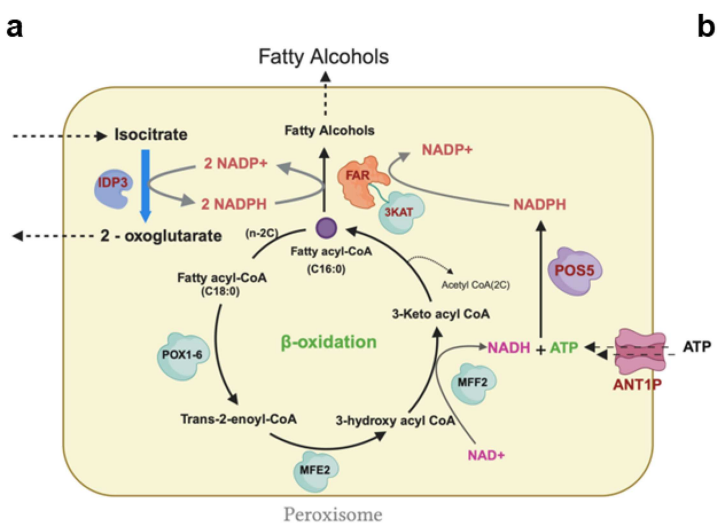

EV (Leu)	+	+	+	+	+	+	-
IDP3	-	+	-	-	-	-	-
Pos5-AKL	-	-	+	-	-	-	-
Pos5-SKL	-	-	-	+	-	-	+
Pos5-BNICL	-	-	-	-	+	-	-
ANT1	-	-	-	-	-	+	+

FIGURE 3 | Redox engineering strategies in the peroxisome. (a) Schematic diagram depicting NADPH enrichment through overexpression of auxiliary enzyme IDP3 and localization of NADH kinase (pos5). (b) Fatty alcohol titer of peroxisomal redox-engineered strains in a shake flask after 7 days of culture. Double asterisks mark a significant change (Student's *t*-test, $p < 0.01$ for double).

it with C-terminal PTS1 tags AKL, SKL, and BNICL, resulting in strains FS116, FS117, and FS118 in the FS106 background strain, respectively. The strains expressing a peroxisome-localized NADH kinase showed increased fatty alcohol production, presumably by enhancing the co-factor supply specifically in the peroxisome. Strain FS117 produced the highest fatty alcohol of 1.45 g/L after 7 days of batch flask fermentation (Figure 3b). In addition, we have also observed that NADH kinase localization has increased the secretion of free fatty acids such as palmitic acid (C16:0) and stearic acid (C18:0) in strain FS117 (Supporting Information S1: Figure S4). GC-FID was used to quantify the secreted fatty acid from the dodecane overlay after 7 days of flask culture (Supporting Information S1: Figure S5a). Further, to increase the production of compartmentalized NADPH from ATP in peroxisomes, we overexpressed the peroxisomal ATP transporter ANT1 alone (strain FS119) and co-expressed ANT1 with *tylPos5* fused to SKL (strain FS120), which resulted in an altered C18:1 distribution in fatty alcohol profile (Figure 3b). However, the strains FS119 and FS120 did not enhance the fatty alcohols production. Instead, titers decreased during episomal expression of the ANT1 transporter, and this strategy was not pursued further.

3.4 | Peroxisome Biogenesis and Precursor Flux Improvement in Fatty Alcohol Producing Strain

Peroxisome proliferation occurs from existing mature peroxisomes via growth and fission or could arise from de novo biogenesis derived from the Endoplasmic Reticulum (ER) (Akşit and van der Klei 2018). To date, over 35 peroxins (PEX) were identified for the biogenesis of peroxisomes in yeast cells. *PEX* genes play a critical role in biogenesis, maintenance, regulation, and abundance of peroxisomes. To enhance the capacity for fatty alcohols production within peroxisome organelles, we targeted PEX11p and PEX16p aiming to modulate their morphology. Studies have shown that the overexpression of PEX11 promotes the abundance of peroxisomes and formation of small peroxisomes (Dulermo et al. 2015; X. Li and Gould 2002; Marshall et al. 1995; Tam et al. 2003). Whereas, the overexpression of PEX16 resulted in a reduced number of larger peroxisomes (Eitzen et al. 1997; Tam et al. 2003; Titorenko and Mullen 2006) (Figure 4a). In this study, the strain FS122 overexpressing PEX16 has increased the fatty alcohol titer to 996 mg/L compared to strain FS121 overexpressing PEX11. Strain FS121 had a modest decrease in titer, which would suggest PEX16-induced peroxisomal changes that benefit peroxisomal fatty alcohol production.

Next, we increased the precursor for fatty alcohol production by enhancing the accumulation of free fatty acid in cytosol. First, we created a strain FS123 that overexpresses the ATP citrate lyase (ACL), which catalyzes the conversion from citrate to generate cytosolic acetyl-CoA, which in turn leads to increased lipid flux (H. Zhang et al. 2014). Second, we created a strain FS124 overexpressing triacylglycerol lipase (TGL4) to enable the lipolysis of stored triacylglycerol (TAG) and release free fatty acids in cytosol (Ledesma-Amaro et al. 2016) (Figure 4b). We hypothesized that the accumulation of free fatty acids drives increased transport into the peroxisome for fatty alcohol production. Indeed, the strains FS123 and FS124 showed significantly improved production of fatty acid and fatty alcohol (Figure 4c). In addition, we constructed multiple copies of 3KAT fusion in *Y. lipolytica* to enhance the production of fatty alcohols. We investigated the impact of introducing one (FS125) or two (FS126) additional copies of 3KAT-GS-TaFAR into the FS117 strain background. However, we found the copy number had little impact on fatty alcohol production (Figure 4c).

3.5 | Fed-Batch Fermentation for Fatty Alcohol Production From Bioreactor

Finally, we demonstrated the scalability of peroxisome-engineered *Y. lipolytica* for the compartmentalized production of fatty alcohols from shake flask culture to a 2 L bioreactor in

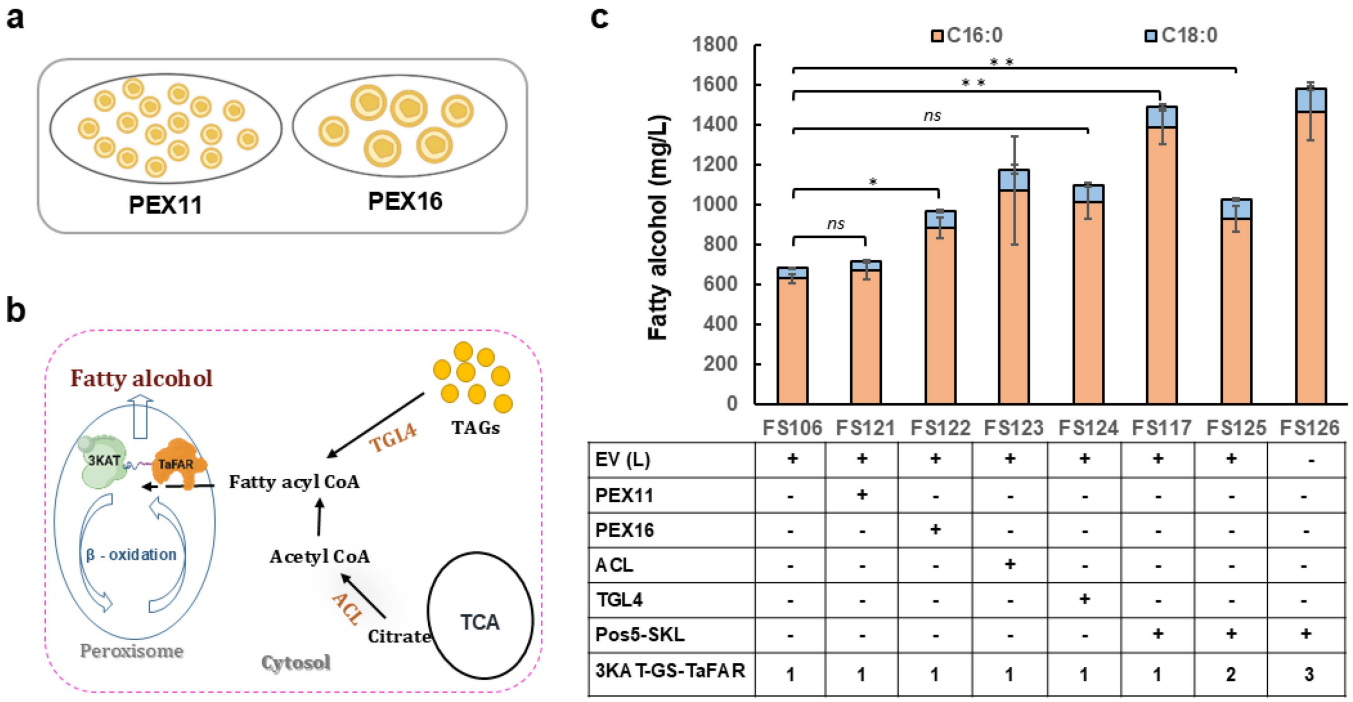

	FS106	FS121	FS122	FS123	FS124	FS117	FS125	FS126
EV (L)	+	+	+	+	+	+	+	-
PEX11	-	+	-	-	-	-	-	-
PEX16	-	-	+	-	-	-	-	-
ACL	-	-	-	+	-	-	-	-
TGL4	-	-	-	-	+	-	-	-
Pos5-SKL	-	-	-	-	-	+	+	+
3KAT-GS-TaFAR	1	1	1	1	1	1	2	3

FIGURE 4 | Additional engineering strategies to improve precursor supply and peroxisome biogenesis (a) Schematic diagram depicting the impact of PEX11 and PEX16 overexpression on peroxisome biogenesis. (b) Increasing free fatty acid accumulation by overexpression of ACL and TGL4. (c) Fatty alcohol production from strains increases precursor supply, copy numbers, and organelle biogenesis. Single and double asterisks mark significant change, whereas *ns* is non-significant (Student's *t*-test, $p < 0.05$ for single and $p < 0.01$ for double).

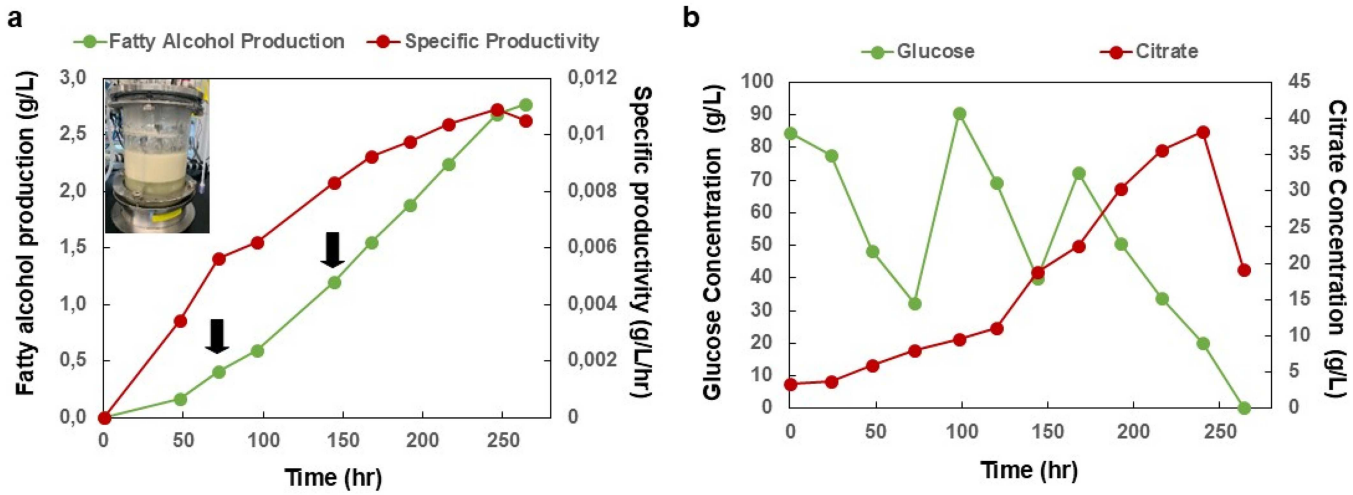

FIGURE 5 | Fed-batch fermentation of strain FS117 for fatty alcohol production in Bioflo320: (a) Total fatty alcohol production and specific productivity. Arrows represent the 80 g glucose spike at 72 and 144 h. (b) Measurement of glucose concentration and citrate accumulation throughout the fermentation.

an Eppendorf Bioflo320 system. We tested the best producer strain FS117 for fatty alcohol production in fed-batch fermentation for 260 h with controlled pH of 5.0 and DO of 40% throughout the bioreactor cultivation period (Supporting Information S1: Figure S6). To keep the cells in active lipogenesis and prevent the exhaustion of carbon source glucose, we spiked two rounds of 80 g glucose at the intervals of 3 days of fermentation at 72 and 144 h. Our results show that fatty alcohol production was improved in bioreactor to 2.77 g/L of total fatty alcohol, of which was 91% hexadecanol (C16:0) and 9% octadecanol (C18:0) (Figure 5a). Hence, peroxisomal localization significantly enhanced fatty alcohol production in *Y. lipolytica* and we were able to achieve hexadecanol titers of 2.53 g/L, the highest reported titers of C16:0 in *Y. lipolytica* till date (Table 1). During the bioreactor run, the strain reached a maximum specific productivity of 10.8 mg/L/h for fatty alcohol production, with a hexadecanol yield of 10.5 mg/g glucose consumed during fermentation. Glucose utilization and citrate accumulation were measured throughout the culture and were completely utilized by the end of the bioreactor run. Citrate was steadily accumulated throughout the fermentation while glucose was present in the bioreactor. Once glucose was depleted,

TABLE 1 | Fatty alcohol distribution profile from fed-batch fermentation.

Alcohols	Fatty alcohol titer (g/L)	Production rate (mg/L/h)	Fatty alcohol distribution (%)
Hexadecanol (C16:0)	2.53 ± 0.05	9.7	91
Octadecanol (C18:0)	0.23 ± 0.006	0.88	9
Total	2.77 ± 0.05	10.8	100

cells began to utilize the accumulated citrate as the carbon source after 240 h of fermentation (Figure 5b). Dry cell weight was measured throughout the bioreactor run (Supporting Information S1: Figure S7).

4 | Discussion

Pathway compartmentalization in subcellular organelles has been a successful approach for substrate channeling to enhance the production of various metabolite targets such as squalene, isobutanol, isopentanol, itaconic acid, and fatty acids (Avalos et al. 2013; Blazeck, Miller, et al. 2014; Dusséaux et al. 2020; G.-S. Liu et al. 2020; Ma et al. 2021). Until now, several studies on compartmentalized production of fatty alcohols were mainly focused on successful localization of biosynthetic pathways into the peroxisome using PTS1 tags in host cells (Sheng et al. 2016; Zhai et al. 2023; Y. J. Zhou et al. 2016). However, fatty alcohol production in peroxisomes was constrained by the pathway enzyme localization efficiency within the organelle and the shortage of cofactor availability in the peroxisomes. In this study, we systemically investigated and harnessed the capacity of *Y. lipolytica* peroxisomes to increase the production of fatty alcohols.

We first localized fatty alcohol biosynthetic enzymes to the peroxisome using various PTS1 family signal sequences and measured the fatty alcohol production (Supporting Information S1: Figure S2). For the first time, a novel peroxisome localization protein 3KAT was identified for its localization property into peroxisomes and its efficiency was tested using GFP as the reporter protein (Figure 2C). 3KAT (also known as POT1) is a promiscuous native peroxisomal enzyme that has broad chain-length specificity, catalyzing the last step of the beta-oxidation cycle for fatty acid chain shortening in peroxisome of *Y. lipolytica* (Beopoulos et al. 2008; Berninger et al. 1993). Enzyme fusions have been a successful approach to promote spatial clustering of biosynthetic pathway enzymes and channel the metabolic flux to increase the target products production (X. Chen et al. 2013; H.-H. Liu et al. 2019; Rabeharindranto et al. 2019; Somasundaram et al. 2017). Thus, we implemented the enzyme fusion strategy toward the peroxisome to increase the compartmentalized production of fatty alcohols by keeping TaFAR in close proximity to 3KAT. The fatty acyl-CoA chains produced by the 3KAT enzyme at every cycle of beta-oxidation act as a direct substrate for TaFAR to produce fatty alcohols. Expression of 3KAT fused with TaFAR using a flexible linker in strain FS106 led to a significant improvement of fatty alcohol production of 693 mg/L, which was higher than simply using PTS1 signal peptides to localize TaFAR to the peroxisome (Figure 2b). Additionally, a PTS2 signal sequence tag was identified at the N-terminus region of 3KAT and its localization efficiency was tested with TaFAR in peroxisomes by measuring the fatty alcohol titer change (Figure 2d). Recently published work provided a comprehensive model of PTS2 protein import mechanism in peroxisome, which chaperone PEX39 extracts PEX7 from cytosol and helps to reload PEX7 to new receptor (Skowyra and Rapoport 2025).

Next, we identified that the presence of limited reducing power in the peroxisomes is the rate-limiting condition for the fatty alcohol production (Supporting Information S1: Figure S3). The peroxisome membrane is permeable to metabolites less than 400 Da (Plett et al. 2020; Stehlik et al. 2014), thereby preventing import of cytosolic NADPH. Here we show that the auxiliary enzyme IDP3 is the major supplier of reducing power present in the peroxisome (Henke et al. 1998). The enriched metabolic flux toward the peroxisome for fatty alcohol production results in the shortage of redox cofactors. Therefore, to address the limitation of NADPH in peroxisomes, we first constructed the strain FS113 to overexpress the native auxiliary enzyme IDP3. The increased NADPH supply in peroxisome organelles resulted in an increased final fatty alcohol titer of 1.25 g/L. Every cycle of beta-oxidation in the peroxisome produces one mole of NADH. To take advantage of beta-oxidation-supplied NADH and to increase the peroxisomal NADPH pool, a NADH kinase enzyme was localized to the peroxisome to compartmentalize the direct phosphorylation of NADH and ATP into NADPH. The truncated version of NADH kinase enzyme, tylPos5 from mitochondria, was localized to the peroxisome using the PTS1 tag to increase the peroxisomal localized NADPH concentration in the strain FS117. When compared to the strain FS106 harboring only the 3KAT fusion, strains FS113 and FS117 harboring both 3KAT fusions and redox engineering strategies showed 1.8- and 2.1-fold increases in fatty alcohols production, respectively. Alternative methods used for enhancing NADPH in bacteria, such as the use of a transhydrogenase UdhA (Sanchez et al. 2006; Cai et al. 2017) may not be as promising in a peroxisomally compartmentalized pathway as $NADP^+$/NADPH cannot freely cross the peroxisomal lipid bilayer due to their size and charge. Consequently, the availability of the $NADP^+$ pool within the peroxisome is likely to be a rate-limiting factor for UdhA-mediated NADPH generation.

Recent work conducted in peroxisome engineering for fatty alcohols production in *S. cerevisiae* reported a total fatty alcohol titer of 282 mg/L from 20 g/L glucose in batch culture, with C16:0 fatty alcohol estimated to 50% of total alcohol titer. This corresponds to a yield of 7 mg/g glucose (N. Gao et al. 2022). In comparison, our study on the engineering of the peroxisome of *Y. lipolycia* has achieved the highest reported hexadecanol C16:0 fatty alcohol titer of 1.35 g/L in strain FS117, which resulted in a yield of 16.87 mg/g glucose consumed in the batch culture. This enhanced production of higher C16:0 fatty alcohol distribution is likely partly attributed to the enzyme TaFAR specificity toward C16:0 fatty acids (Hu et al. 2020). Additionally, the strains overexpressing the peroxisomally targeted *Pos5*

TABLE 2 | Comparison of peroxisomal compartmentalization strategies for fatty alcohol production across different host organisms.

Organisms	Organelle	Strategy	Sub	Fatty alcohols	Titer	Yield	References
Saccharomyces cerevisiae	Peroxisome	TaFAR localization, Pex7 overexpression	Glu	C10:0, C12:0, C16:0	0.83 g/L^{bsf} 1.3 g/L^{fbsf}	41.5 mg/g bsf 43.3 mg/g fbsf	Sheng et al. (2016)
S. cerevisiae	Peroxisome	FaCoAR localization	Glu	C14:0, C16:0, C16:1, C18:0, C18:1	193 mg/L^{bsf}	6.43 mg/g bsf	Y. J. Zhou et al. (2016)
S. cerevisiae	Peroxisome	MaFAR1 localization, improved acyl-CoA and NADPH supply	Glu	C14:0, C16:0, C16:1, C18:0, C18:1	282 mg/L^{bsf}	14.1 mg/g bsf	N. Gao et al. (2022)
Pichia pastoris	Cytosol and peroxisome	MmFAR and ScADH5, methanol assimilation, enhanced precursor supply	MeOH	C16:0, C16:1, C18:0, C18:1	1.9 g/L^{fbsf} 5.6 g/L^{fbr}	16 mg/g fbsf 8 mg/g fbr	Shen et al. (2024)
Ogataea polymorpha	Peroxisome	TaFAR localization, Peroxisomal NADPH supply, formaldehyde assimilation	MeOH	C16:0, C18:0 C18:1, C18:2	3.6 g/L^{fbr}	16 mg/g fbr	Zhai et al. (2023)
Y. lipolyica	Peroxisome	TaFAR localization, peroxisome biogenesis, enhanced NADPH and precursors supply	Glu	C16:0, C18:0	1.45 g/L^{bsf} 2.77 g/L^{fbr}	18.12 mg/g bsf 11.54 mg/g fbr	This study

Abbreviations: bsf, batch shake flask; fbr, fed-batch bioreactor; fbsf, fed-batch shake flask.

NADH kinase showed secretion of free fatty acids such as C16:0 Hexadecanoic acid and C18:0 Octadecanoic acid in the dodecane overlay (Supporting Information S1: Figure S4a), for reasons that remain elusive.

The robustness of manipulating organelles and leveraging them as micro-factories has elevated the fatty alcohol titer in this study (Table 2). Furthermore, additional engineering strategies such as increasing available fatty alcohols precursor supply from cytosol were demonstrated in fatty alcohol producing strains have focused on enriching the free fatty acid flux and increases the copy number of the enzyme fusion system for optimal fatty alcohols production (Figure 4c). The strain developed in this study was compared with *S. cerevisiae* and other hosts for peroxisomal fatty alcohol production, including titer, strategies, and product compositions, as summarized in Table 2. This comparison shows that while titers in fed-batch are similar but lower, our batch culture titers and yields are amongst the highest reported, and represent a significant step forward in peroxisomal fatty alcohol production. While other studies noted significant regulatory impacts by localizing the PHB synthesis pathway (Xiao et al. 2025) to the peroxisome while changing to acetate-based media, we noted no significant changes to cell growth or substrate consumption in our work. Future studies may more comprehensively examine the regulatory effects of pathway compartmentalization in our systems; however, the effects are likely to be specific to the pathways involved.

In conclusion, we show that the spatial localization of fatty alcohol biosynthetic enzymes into the peroxisome increases fatty alcohol production in a compartmentalized environment and could prevent the loss of flux via competing reactions. We extensively harnessed *Y. lipolytica* peroxisomes in this study to overcome the localization efficiency, redirecting metabolic flux, enriched organelle redox, modulating organelle biogenesis, and increased precursor flux pool. The above subcellular organelle engineering strategies implemented in this work have transformed the peroxisome into an ideal micro-factory, achieving the highest reported C16:0 hexadecanol fatty alcohols titers from *Y. lipolytica*. This work lays the foundation for future studies aiming to produce chain length-specific fatty alcohols through protein engineering strategies targeting 3KATs, FARs, or other enzymes involved in the beta-oxidation cycle. Furthermore, the approaches used to harness the peroxisomes in this study can be applied to other subcellular organelles, enabling the spatial localization of biosynthetic pathways within natural or synthetic compartments in living cells and potentially enhancing the production of biomolecules.

Author Contributions

Sivachandiran Somasundaram: conceptualization, experiments, data curation, formal analysis, investigation, methodology, validation, visualization, writing – original draft, writing – review and editing. **Ayushi Agrawal:** experiment, validation, writing – review and editing. **Philip Gitman:** experiment, validation, writing – review and editing. **Michael Spagnuolo:** validation, resources, formal analysis, investigation, methodology. **Mark Blenner:** conceptualization, funding acquisition, project administration, supervision, writing – review and editing.

Acknowledgments

The authors would like to thank Vijay Ganesan, Richa Guleria, Patrick Beardslee, and Christopher Nauman for their insightful comments

during experiments and manuscript revision. The authors would also like to acknowledge Dr. Sylvain Le Marchand for the help provided for the microscopy visualization study. This work was supported by NSF CBET-1706134 (M.B.) and also by an Early Career Faculty Grant from NASA's Space Technology Research Grants Program (M.B.) (Grant no. NNX15AU46G).

Conflicts of Interest

Work from this manuscript is claimed under international patent application number PCT/US2023/071236. The authors declare no conflicts of interest.

References

Akhtar, M. K., N. J. Turner, and P. R. Jones. 2013. "Carboxylic Acid Reductase Is a Versatile Enzyme for the Conversion of Fatty Acids into Fuels and Chemical Commodities." *Proceedings of the National Academy of Sciences of the United States of America* 110: 87–92. https://doi.org/10.1073/pnas.1216516110.

Akşit, A., and I. J. van der Klei. 2018. "Yeast Peroxisomes: How Are They Formed and How Do They Grow?" *International Journal of Biochemistry & Cell Biology* 105: 24–34. https://doi.org/10.1016/j.biocel.2018.09.019.

Avalos, J. L., G. R. Fink, and G. Stephanopoulos. 2013. "Compartmentalization of Metabolic Pathways in Yeast Mitochondria Improves the Production of Branched-Chain Alcohols." *Nature Biotechnology* 31: 335–341. https://doi.org/10.1038/nbt.2509.

Baker, J. J., J. Shi, S. Wang, et al. 2025. "ML-Enhanced Peroxisome Capacity Enables Compartmentalization of Multienzyme Pathway." *Nature Chemical Biology* 21: 727–735. https://doi.org/10.1038/s41589-024-01759-2.

Beopoulos, A., Z. Mrozova, F. Thevenieau, et al. 2008. "Control of Lipid Accumulation in the Yeast *Yarrowia lipolytica*." *Applied and Environmental Microbiology* 74: 7779–7789. https://doi.org/10.1128/AEM.01412-08.

Berninger, G., R. Schmidtchen, G. Casel, et al. 1993. "Structure and Metabolic Control of the *Yarrowia lipolytica* Peroxisomal 3-Oxoacyl-CoA-Thiolase Gene." *European Journal of Biochemistry* 216: 607–613. https://doi.org/10.1111/j.1432-1033.1993.tb18180.x.

Bi, K., W. Wang, D. Tang, et al. 2024. "Engineering Sub-Organelles of a Diploid *Saccharomyces cerevisiae* to Enhance the Production of 7-Dehydrocholesterol." *Metabolic Engineering* 84: 169–179. https://doi.org/10.1016/j.ymben.2024.06.011.

Blazeck, J., A. Hill, L. Liu, et al. 2014. "Harnessing *Yarrowia lipolytica* Lipogenesis to Create a Platform for Lipid and Biofuel Production." *Nature Communications* 5: 3131. https://doi.org/10.1038/ncomms4131.

Blazeck, J., J. Miller, A. Pan, et al. 2014. "Metabolic Engineering of *Saccharomyces cerevisiae* for Itaconic Acid Production." *Applied Microbiology and Biotechnology* 98: 8155–8164. https://doi.org/10.1007/s00253-014-5895-0.

Bruder, S., E. J. Moldenhauer, R. D. Lemke, R. Ledesma-Amaro, and J. Kabisch. 2019. "Drop-In Biofuel Production Using Fatty Acid Photodecarboxylase From Chlorella Variabilis in the Oleaginous Yeast *Yarrowia lipolytica*." *Biotechnology for Biofuels* 12: 202. https://doi.org/10.1186/s13068-019-1542-4.

Bryksin, A. V., and I. Matsumura. 2010. "Overlap Extension PCR Cloning: A Simple and Reliable Way to Create Recombinant Plasmids." *Biotechniques* 48: 463–465. https://doi.org/10.2144/000113418.

Cai, D., P. He, X. Lu, et al. 2017. "A Novel Approach to Improve Poly-γ-Glutamic Acid Production by NADPH Regeneration in *Bacillus licheniformis* WX-02." *Scientific Reports* 7: 43404. https://doi.org/10.1038/srep43404.

Chen, L., W. Xiao, M. Yao, Y. Wang, and Y. Yuan. 2023. "Compartmentalization Engineering of Yeasts to Overcome Precursor Limitations and Cytotoxicity in Terpenoid Production." *Frontiers in Bioengineering and Biotechnology* 11: 1132244. https://doi.org/10.3389/fbioe.2023.1132244.

Chen, X., J. L. Zaro, and W.-C. Shen. 2013. "Fusion Protein Linkers: Property, Design and Functionality." *Advanced Drug Delivery Reviews* 65: 1357–1369. https://doi.org/10.1016/j.addr.2012.09.039.

Cordova, L. T., J. Butler, and H. S. Alper. 2020. "Direct Production of Fatty Alcohols From Glucose Using Engineered Strains of *Yarrowia lipolytica*." *Metabolic Engineering Communications* 10: e00105. https://doi.org/10.1016/j.mec.2019.e00105.

D'Espaux, L., A. Ghosh, W. Runguphan, et al. 2017. "Engineering High-Level Production of Fatty Alcohols by *Saccharomyces cerevisiae* From Lignocellulosic Feedstocks." *Metabolic Engineering* 42: 115–125. https://doi.org/10.1016/j.ymben.2017.06.004.

Dulermo, R., T. Dulermo, H. Gamboa-Meléndez, F. Thevenieau, and J.-M. Nicaud. 2015. "Role of Pex11p in Lipid Homeostasis in *Yarrowia lipolytica*." *Eukaryotic Cell* 14: 511–525. https://doi.org/10.1128/EC.00051-15.

Dusséaux, S., W. T. Wajn, Y. Liu, C. Ignea, and S. C. Kampranis. 2020. "Transforming Yeast Peroxisomes into Microfactories for the Efficient Production of High-Value Isoprenoids." *Proceedings of the National Academy of Sciences of the United States of America* 117: 31789–31799. https://doi.org/10.1073/pnas.2013968117.

Eitzen, G. A., R. K. Szilard, and R. A. Rachubinski. 1997. "Enlarged Peroxisomes Are Present in Oleic Acid–Grown *Yarrowia lipolytica* Overexpressing the *PEX16* Gene Encoding an Intraperoxisomal Peripheral Membrane Peroxin." *Journal of Cell Biology* 137: 1265–1278. https://doi.org/10.1083/jcb.137.6.1265.

Fillet, S., J. Gibert, B. Suárez, A. Lara, C. Ronchel, and J. L. Adrio. 2015. "Fatty Alcohols Production by Oleaginous Yeast." *Journal of Industrial Microbiology and Biotechnology* 42: 1463–1472. https://doi.org/10.1007/s10295-015-1674-x.

Gao, D., S. Smith, M. Spagnuolo, G. Rodriguez, and M. Blenner. 2018. "Dual CRISPR-Cas9 Cleavage Mediated Gene Excision and Targeted Integration in *Yarrowia lipolytica*." *Biotechnology Journal* 15: e1700590. https://doi.org/10.1002/biot.201700590.

Gao, J., and Y. J. Zhou. 2019. "Repurposing Peroxisomes for Microbial Synthesis for Biomolecules." *Methods in Enzymology* 617: 83–111. https://doi.org/10.1016/bs.mie.2018.12.004.

Gao, N., J. Gao, W. Yu, S. Kong, and Y. J. Zhou. 2022. "Spatial–Temporal Regulation of Fatty Alcohol Biosynthesis in Yeast." *Biotechnology for Biofuels and Bioproducts* 15: 141. https://doi.org/10.1186/s13068-022-02242-7.

Gao, Q., J.-L. Yang, X.-R. Zhao, et al. 2020. "*Yarrowia lipolytica* as a Metabolic Engineering Platform for the Production of Very-Long-Chain Wax Esters." *Journal of Agricultural and Food Chemistry* 68: 10730–10740. https://doi.org/10.1021/acs.jafc.0c04393.

Gatter, M., A. Förster, K. Bär, et al. 2014. "A Newly Identified Fatty Alcohol Oxidase Gene Is Mainly Responsible for the Oxidation of Long-Chain ω-Hydroxy Fatty Acids in *Yarrowia lipolytica*." *FEMS Yeast Research* 14: 858–872. https://doi.org/10.1111/1567-1364.12176.

Hammer, S. K., and J. L. Avalos. 2017. "Harnessing Yeast Organelles for Metabolic Engineering." *Nature Chemical Biology* 13: 823–832. https://doi.org/10.1038/nchembio.2429.

Henke, B., W. Girzalsky, V. Berteaux-Lecellier, and R. Erdmann. 1998. "IDP3 Encodes a Peroxisomal NADP-Dependent Isocitrate Dehydrogenase Required for the β-Oxidation of Unsaturated Fatty Acids." *Journal of Biological Chemistry* 273: 3702–3711. https://doi.org/10.1074/jbc.273.6.3702.

Hofvander, P., T. T. P. Doan, and M. Hamberg. 2011. "A Prokaryotic Acyl-CoA Reductase Performing Reduction of Fatty Acyl-CoA to Fatty

Alcohol." *FEBS Letters* 585: 3538–3543. https://doi.org/10.1016/j.febslet.2011.10.016.

Hu, Y., Z. Zhu, D. Gradischnig, M. Winkler, J. Nielsen, and V. Siewers. 2020. "Engineering Carboxylic Acid Reductase for Selective Synthesis of Medium-Chain Fatty Alcohols in Yeast." *Proceedings of the National Academy of Sciences of the United States of America* 117: 22974–22983. https://doi.org/10.1073/pnas.2010521117.

Keim, W. 2013. "Oligomerization of Ethylene to α-Olefins: Discovery and Development of the Shell Higher Olefin Process (SHOP)." *Angewandte Chemie International Edition* 52: 12492–12496. https://doi.org/10.1002/anie.201305308.

Ledesma-Amaro, R., R. Dulermo, X. Niehus, and J.-M. Nicaud. 2016. "Combining Metabolic Engineering and Process Optimization to Improve Production and Secretion of Fatty Acids." *Metabolic Engineering* 38: 38–46. https://doi.org/10.1016/j.ymben.2016.06.004.

Li, M. Z., and S. J. Elledge. 2012. "SLIC: A Method for Sequence- and Ligation-Independent Cloning." *Methods in Molecular Biology (Clifton, N.J.)* 852: 51–59. https://doi.org/10.1007/978-1-61779-564-0_5.

Li, X., and S. J. Gould. 2002. "PEX11 Promotes Peroxisome Division Independently of Peroxisome Metabolism." *Journal of Cell Biology* 156: 643–651. https://doi.org/10.1083/jcb.200112028.

Liu, A., X. Tan, L. Yao, and X. Lu. 2013. "Fatty Alcohol Production in Engineered *E. coli* Expressing Marinobacter Fatty Acyl-CoA Reductases." *Applied Microbiology and Biotechnology* 97: 7061–7071. https://doi.org/10.1007/s00253-013-5027-2.

Liu, G.-S., T. Li, W. Zhou, et al. 2020. "The Yeast Peroxisome: A Dynamic Storage Depot and Subcellular Factory for Squalene Overproduction." *Metabolic Engineering* 57: 151–161. https://doi.org/10.1016/j.ymben.2019.11.001.

Liu, H.-H., C. Wang, X.-Y. Lu, H. Huang, Y. Tian, and X.-J. Ji. 2019. "Improved Production of Arachidonic Acid by Combined Pathway Engineering and Synthetic Enzyme Fusion in *Yarrowia lipolytica*." *Journal of Agricultural and Food Chemistry* 67: 9851–9857. https://doi.org/10.1021/acs.jafc.9b03727.

Ma, Y., J. Li, S. Huang, and G. Stephanopoulos. 2021. "Targeting Pathway Expression to Subcellular Organelles Improves Astaxanthin Synthesis in *Yarrowia lipolytica*." *Metabolic Engineering* 68: 152–161. https://doi.org/10.1016/j.ymben.2021.10.004.

Marshall, P. A., Y. I. Krimkevich, R. H. Lark, J. M. Dyer, M. Veenhuis, and J. M. Goodman. 1995. "Pmp27 Promotes Peroxisomal Proliferation." *Journal of Cell Biology* 129: 345–355. https://doi.org/10.1083/jcb.129.2.345.

Mehrer, C. R., M. R. Incha, M. C. Politz, and B. F. Pfleger. 2018. "Anaerobic Production of Medium-Chain Fatty Alcohols via a β-Reduction Pathway." *Metabolic Engineering* 48: 63–71. https://doi.org/10.1016/j.ymben.2018.05.011.

Metz, J. G., M. R. Pollard, L. Anderson, T. R. Hayes, and M. W. Lassner. 2000. "Purification of a Jojoba Embryo Fatty Acyl-Coenzyme A Reductase and Expression of Its cDNA in High Erucic Acid Rapeseed." *Plant Physiology* 122: 635–644. https://doi.org/10.1104/pp.122.3.635.

Munkajohnpong, P., C. Kesornpun, S. Buttranon, J. Jaroensuk, N. Weeranoppanant, and P. Chaiyen. 2020. "Fatty Alcohol Production: An Opportunity of Bioprocess." *Biofuels, Bioproducts and Biorefining* 14: 986–1009. https://doi.org/10.1002/bbb.2112.

Noweck, K., and W. Grafahrend. 2006. "Fatty Alcohols." In *Ullmann's Encyclopedia of Industrial Chemistry*. Wiley. https://doi.org/10.1002/14356007.a10_277.pub2.

Outten, C. E. 2003. "A Novel NADH Kinase Is the Mitochondrial Source of NADPH in *Saccharomyces cerevisiae*." *EMBO Journal* 22: 2015–2024. https://doi.org/10.1093/emboj/cdg211.

Plett, A., L. Charton, and N. Linka. 2020. "Peroxisomal Cofactor Transport." *Biomolecules* 10: 1174. https://doi.org/10.3390/biom10081174.

Pollard, M. R., T. McKeon, L. M. Gupta, and P. K. Stumpf. 1979. "Studies on Biosynthesis of Waxes by Developing Jojoba Seed. II. the Demonstration of Wax Biosynthesis by Cell-Free Homogenates." *Lipids* 14: 651–662. https://doi.org/10.1007/BF02533451.

Pomraning, K. R., Y.-M. Kim, C. D. Nicora, et al. 2016. "Multi-Omics Analysis Reveals Regulators of the Response to Nitrogen Limitation in *Yarrowia lipolytica*." *BMC Genomics* 17: 138. https://doi.org/10.1186/s12864-016-2471-2.

Rabeharindranto, H., S. Castaño-Cerezo, T. Lautier, et al. 2019. "Enzyme-Fusion Strategies for Redirecting and Improving Carotenoid Synthesis in *S. cerevisiae*." *Metabolic Engineering Communications* 8: e00086. https://doi.org/10.1016/j.mec.2019.e00086.

Rottensteiner, H., and F. L. Theodoulou. 2006. "The Ins and Outs of Peroxisomes: Co-Ordination of Membrane Transport and Peroxisomal Metabolism." *Biochimica et Biophysica Acta (BBA)-Molecular Cell Research* 1763: 1527–1540. https://doi.org/10.1016/j.bbamcr.2006.08.012.

Sanchez, A. M., J. Andrews, I. Hussein, G. N. Bennett, and K. Y. San. 2006. "Effect of Overexpression of a Soluble Pyridine Nucleotide Transhydrogenase (UdhA) on the Production of Poly(3-Hydroxybutyrate) in *Escherichia coli*." *Biotechnology Progress* 22, no. 2: 420–425.

Schwartz, C., M. Shabbir-Hussain, K. Frogue, M. Blenner, and I. Wheeldon. 2017. "Standardized Markerless Gene Integration for Pathway Engineering in *Yarrowia lipolytica*." *ACS Synthetic Biology* 6: 402–409. https://doi.org/10.1021/acssynbio.6b00285.

Schwartz, C., and I. Wheeldon. 2018. "CRISPR-Cas9-Mediated Genome Editing and Transcriptional Control in *Yarrowia lipolytica*." *Methods in Molecular Biology (Clifton, N.J.)* 1772: 327–345. https://doi.org/10.1007/978-1-4939-7795-6_18.

Shen, Y., P. Cai, L. Gao, X. Wu, L. Yao, and Y. J. Zhou. 2024. "Engineering High Production of Fatty Alcohols From Methanol by Constructing Coordinated Dual Biosynthetic Pathways." *Bioresource Technology* 412: 131396. https://doi.org/10.1016/j.biortech.2024.131396.

Sheng, J., J. Stevens, and X. Feng. 2016. "Pathway Compartmentalization in Peroxisome of *Saccharomyces cerevisiae* to Produce Versatile Medium Chain Fatty Alcohols." *Scientific Reports* 6: 26884. https://doi.org/10.1038/srep26884.

Skowyra, M. L., and T. A. Rapoport. 2025. "Import Mechanism of Peroxisomal Proteins With an N-Terminal Signal Sequence." *Nature Cell Biology* 27: 948–958. https://doi.org/10.1038/s41556-025-01662-5.

Somasundaram, S., K.-N. T. Tran, S. Ravikumar, and S. H. Hong. 2017. "Introduction of Synthetic Protein Complex Between *Pyrococcus horikoshii* Glutamate Decarboxylase and *Escherichia coli* GABA Transporter for the Improved Production of GABA." *Biochemical Engineering Journal* 120: 1–6. https://doi.org/10.1016/j.bej.2016.12.020.

Spagnuolo, M., A. Yaguchi, and M. Blenner. 2019. "Oleaginous Yeast for Biofuel and Oleochemical Production." *Current Opinion in Biotechnology* 57: 73–81. https://doi.org/10.1016/j.copbio.2019.02.011.

Stehlik, T., B. Sandrock, J. Ast, and J. Freitag. 2014. "Fungal Peroxisomes as Biosynthetic Organelles." *Current Opinion in Microbiology* 22: 8–14. https://doi.org/10.1016/j.mib.2014.09.011.

Sweetlove, L. J., and A. R. Fernie. 2018. "The Role of Dynamic Enzyme Assemblies and Substrate Channelling in Metabolic Regulation." *Nature Communications* 9: 2136. https://doi.org/10.1038/s41467-018-04543-8.

Tam, Y. Y. C., J. C. Torres-Guzman, F. J. Vizeacoumar, et al. 2003. "Pex11-Related Proteins in Peroxisome Dynamics: A Role for the Novel Peroxin Pex27p in Controlling Peroxisome Size and Number in *Saccharomyces cerevisiae*." *Molecular Biology of the Cell* 14: 4089–4102. https://doi.org/10.1091/mbc.e03-03-0150.

Titorenko, V. I., and R. T. Mullen. 2006. "Peroxisome Biogenesis: The Peroxisomal Endomembrane System and the Role of the ER." *Journal of Cell Biology* 174: 11–17. https://doi.org/10.1083/jcb.200604036.

Wang, G., X. Xiong, R. Ghogare, P. Wang, Y. Meng, and S. Chen. 2016. "Exploring Fatty Alcohol-Producing Capability of *Yarrowia lipolytica*." *Biotechnology for Biofuels* 9: 107. https://doi.org/10.1186/s13068-016-0512-3.

Xiao, Z., X. Xiong, Y. Sun, M. Tourang, S. Chen, and Y. J. Tang. 2025. "Metabolic Analyses of *Yarrowia lipolytica* for Biopolymer Production Reveals Roadblocks and Strategies for Microbial Utilizing Volatile Fatty Acids as Sustainable Feedstocks." *Bioresource Technology* 417: 131855. https://doi.org/10.1016/j.biortech.2024.131855.

Youngquist, J. T., M. H. Schumacher, J. P. Rose, et al. 2013. "Production of Medium Chain Length Fatty Alcohols From Glucose in *Escherichia coli*." *Metabolic Engineering* 20: 177–186. https://doi.org/10.1016/j.ymben.2013.10.006.

Zhai, X., J. Gao, Y. Li, M. Grininger, and Y. J. Zhou. 2023. "Peroxisomal Metabolic Coupling Improves Fatty Alcohol Production From Sole Methanol in Yeast." *Proceedings of the National Academy of Sciences of the United States of America* 120, no. 12: e2220816120. https://doi.org/10.1073/pnas.2220816120.

Zhang, C., C. Chen, X. Bian, et al. 2024. "Construction of an Orthogonal Transport System for *Saccharomyces cerevisiae* Peroxisome to Efficiently Produce Sesquiterpenes." *Metabolic Engineering* 85: 84–93. https://doi.org/10.1016/j.ymben.2024.07.010.

Zhang, H., L. Zhang, H. Chen, et al. 2014. "Enhanced Lipid Accumulation in the Yeast *Yarrowia lipolytica* by Over-Expression of ATP: Citrate Lyase From *Mus musculus*." *Journal of Biotechnology* 192: 78–84. https://doi.org/10.1016/j.jbiotec.2014.10.004.

Zhang, J.-L., Y.-X. Cao, Y.-Z. Peng, et al. 2019. "High Production of Fatty Alcohols in *Yarrowia lipolytica* by Coordination With Glycolysis." *Science China Chemistry* 62: 1007–1016. https://doi.org/10.1007/s11426-019-9456-y.

Zhou, W., R.-J. Ling, Y.-C. Yang, et al. 2025. "Engineering *Komagataella phaffii* to Produce Lycopene Sustainably From Glucose or Methanol." *Metabolic Engineering* 90: 141–153. https://doi.org/10.1016/j.ymben.2025.03.013.

Zhou, Y. J., N. A. Buijs, Z. Zhu, et al. 2016. "Harnessing Yeast Peroxisomes for Biosynthesis of Fatty-Acid-Derived Biofuels and Chemicals With Relieved Side-Pathway Competition." *Journal of the American Chemical Society* 138: 15368–15377. https://doi.org/10.1021/jacs.6b07394.

Supporting Information

Additional supporting information can be found online in the Supporting Information section.
Supplement file 20250918 Revised Submission.